A&A manuscript no.
(will be inserted by hand later)

Your thesaurus codes are:
11(11.05.2, 11.17.1)

ASTRONOMY
AND
ASTROPHYSICS
1.2.2008

Optically identified QSO absorption systems and galaxy evolution

Ulrich Lindner, Uta Fritze – von Alvensleben, Klaus J. Fricke

Universitätssternwarte, Geismarlandstraße 11, D–37083 Göttingen, Germany

Received 17 August 1995 / Accepted 16 April 1996

Abstract. A comprehensive set of all available magnitudes, colors and redshifts for optically identified QSO absorbers is compiled from the literature. This results in a largely unbiased sample of galaxies at high redshifts, the size of the sample being reasonably large to allow for a first comparison with galaxy evolution models. We use our evolutionary spectral synthesis models describing various spectral types of galaxies with appropriate star formation histories.

For a standard cosmology $H_0 = 50$ km s^{-1} Mpc^{-1}, $\Omega_0 = 1$, we find that all identified QSO absorbers up to a redshift $\simeq 2$ do fall within the evolving range of models which had been shown earlier to give good agreement with nearby galaxies of various spectral types.

The most striking result is that **all spectral types** of galaxies from E through Sd seem to be present in this absorber candidate sample with the bulk of the objects being spirals of type Sa to Sc.

We also show that such kind of high redshift galaxy sample should allow for significant restrictions of the cosmological parameters. While models with $H_0 = 50$ km s^{-1} Mpc^{-1}, $\Omega_0 = 1$ and any redshift of galaxy formation $z_{\rm form} = 5 \ldots 10$ give reasonable agreement with observed luminosities and colors, present data seem to exclude the combination $H_0 = 50$ km s^{-1} Mpc^{-1}, $\Omega_0 = 0.1$. A low Ω_0 together with a value of $H_0 > 50$ might still be viable. Additional data, and in particular observations of absorbing galaxies in more than one passband, are required for further constraints. We realize that the present results depend on the adopted evolutionary models and on the input physics used which might be better constrained by future observations.

Key words: Galaxies: evolution – Quasars: absorption lines – absorption line systems: Optical identification

Send offprint requests to: Ulrich Lindner, Universitätssternwarte, Geismarlandstraße 11, D–37083 Göttingen, Germany, e-mail: ulindner@uni-sw.gwdg.de

1. Introduction

Among others, absorption lines from the doublets of MgII and CIV, damped Lyman α lines (hereafter DLA), and Lyman Limit Systems (hereafter LLS) are seen in the spectra of quasars. By now, interpretations seem to converge to the view that the MgII and CIV doublets arise in extended gaseous halos of intervening galaxies, while DLA's are formed in (proto –) galactic disks (Steidel, 1993).

This picture remained hypothetical until the QSO absorbers, i.e. the galaxies causing the absorption lines were actually detected. Pioneering work in the optical was done by Bergeron & Boissé (1991). By now, there are more than a dozen of publications reporting on optical identifications of QSO absorber systems. Their number increases rapidly. We have compiled all relevant data available to us. Information about the data we use is given in §3 and the sources from which our data are drawn are briefly reported in the appendix[1].

A sample of optically identified QSO absorbers has, at least, two advantages over others, e.g. magnitude limited samples, (i) it is scarcely biased to selection effects with respect to luminosity, surface brightness, radio emission, etc. (cf. Steidel *et al.* 1993, Steidel 1995) and (ii) it gives access to galaxies with high redshifts.

This paper is a first attempt to compare a comprehensive set of magnitudes and colors of optically identified QSO absorbers and absorber candidates with galaxy evolution models. Models are briefly described in §2. The aim of this study is first to investigate the properties of this QSO absorbing galaxy sample (cf. §4) and, second, to show that this kind of high redshift galaxy sample should allow for serious restrictions of cosmological parameters

[1] The appendix is also available in electronic form at the CDS via anonymous ftp to cdsarc.u-strasbg.fr (130.79.128.5) or via http://cdsweb.u-strasbg.fr/Abstract.html

(§4.3). We discuss some problems in §5 and outline future prospects in §6. §7 summarizes our conclusions.

2. Models of galaxy evolution

Here, we only give a brief outline of our galaxy evolution models, which have been described in detail earlier by Fritze – von Alvensleben (1989), Krüger *et al.* (1991) and Fritze – von Alvensleben & Gerhard (1994).

2.1. General description of models

Starting from an initial gas cloud stars are formed continuously in a 1–zone model according to a given star formation law. The distribution of the total astrated mass to discrete stellar masses in the range 0.04 $M_\odot$ ... 85 $M_\odot$ is described by a Scalo (1986) IMF.

Using recent stellar evolutionary tracks for solar metallicity from the Geneva group (Maeder, 1991), the population of the HRD is calculated as a function of time. Synthetic galaxy spectra are obtained by assigning stellar spectral types and luminosity classes to some 40 cells in the HRD and by superimposing observed stellar spectra from Gunn & Stryker's (1983) library weighted by the number of stars present in each cell at a given time. Convolution of synthetic galaxy spectra with filter functions yields absolute magnitudes and colors of the model galaxies.

Basic parameters of this kind of models are the initial mass function (hereafter IMF) and the star formation (hereafter SF) laws. For galaxies of various spectral types, we use different parametrisations of their SF histories following Sandage (1986). While an elliptical galaxy is described by a SF rate declining exponentially in time with a characteristic time scale of 1 Gyr, the SF rate in spiral galaxies is a linear function of the gas content with characteristic time scales ranging from 1, 2, 3, 10 to 16 Gyr for S0, Sa, Sb, Sc and Sd, respectively. Gas recycling due to stellar winds, supernovae and planetary nebula is consistently taken into account.

These SF laws together with a Scalo IMF have been shown to give good agreement with observations of the respective galaxy types in the Virgo cluster and in the field in terms of broad band colors UBVRI, gaseous emission lines, M/L ratios, gas content, etc. (Fritze – von Alvensleben 1989, Krüger *et al.* 1991 & 1995, Fritze – von Alvensleben & Gerhard (1994). Furthermore, we find detailed agreement with Kennicutt's (1992) template galaxy spectra for the various Hubble types.

For comparable characteristic time scales in the SF laws, the time evolution of our model galaxies agrees to within 0.1 mag with Bruzual & Charlot's (1993) models which are based on slightly different stellar evolution tracks. Except for very early phases ($z \geq 1$) we obtain somewhat bluer colors at the largest wavelengths.

It should be stressed that in our context the different **Hubble types** of galaxies as described by their respective SF laws are meant to be **spectral types** rather than morphological types. Only for nearby galaxies the correspondence between morphological types and spectroscopic types has been shown, it remains to be investigated for high redshift galaxies. We have also studied the chemical evolution of individual elements in the interstellar medium (hereafter ISM) for these same SF laws and found satisfactory agreement with observations of MgII– and CIV–systems (Fritze – von Alvensleben *et al.* 1989 & 1991) and with abundances derived for DLA systems as well (Fritze – von Alvensleben 1994) over a redshift range $0 \leq z \leq 4$ for a Scalo–IMF.

It is clear, however, that all the results presented below depend quantitatively on our specific models. Should future observational evidence impose changes, e.g. in the IMF, the SF laws, or in the stellar input tracks, our conclusions may have to be modified appropriately.

To transform time dependent absolute magnitudes into observable apparent magnitudes $m_\lambda(z)$ as a function of redshift a cosmological model has to be specified. Here, we adopt a Friedmann–Lemaître model with vanishing cosmological constant ($\Lambda_0 = 0$), so H_0 and Ω_0 ($= 2q_0$ in the case of $\Lambda_0 = 0$) are the cosmological parameters together with the redshift $z_{\rm form}$ where star formation in our model galaxies is assumed to start.

The relation between redshift and time is given by the standard formula for the *Hubble–time* $T_H(z, H_0, \Omega_0)$. Then, for given (H_0, Ω_0) the age of a galaxy formed at redshift $z_{\rm form}$ is calculated from

$$t_{gal}(z) = T_H(z) - T_H(z_{\rm form}).$$

The relation between redshift and distance is given by the standard formula for the *luminosity distance* $D_L(z, H_0, \Omega_0)$ which is used to calculate the *bolometric distance modulus*

$$BDM(z) = 5\ \log(D_L)\ +\ 25.$$

Finally, the observable apparent magnitude at a wavelength (filter band) λ writes

$$m_\lambda(z) = BDM(z) + k_\lambda(z) + e_\lambda(z) + M_\lambda(0, t_0)$$

with $t_0 = t_{gal}(z = 0)$. The evolutionary correction

$$e_\lambda(z) := M_\lambda(z, t_{gal}(z)) - M_\lambda(z, t_0)$$

takes into account the variation of the galaxy spectrum with time. The cosmological correction

$$k_\lambda(z) := M_\lambda(z, t_0) - M_\lambda(0, t_0)$$

accounts for the influence of the expansion of the Universe.

It is important to stress that both the evolutionary and cosmological corrections do not only depend on the cosmological parameters but also on the spectral type of the galaxies (cf. also Rocca–Volmerange & Guiderdoni, 1988). Before red-shifting our model galaxies, we calibrate their absolute magnitudes M_B to mean luminosities of galaxies in the Virgo cluster as determined by Sandage *et al.* (1985a, 1985b) for the various Hubble types.

2.2. Implications from models

For this paper, apparent magnitudes as a function of redshift are calculated from our models for two different photometric systems. Results of our models for Johnson R and Thuan & Gunn r are presented in Figure 1. Late type galaxies (Sd) not only are significantly fainter than mean early type galaxies (E) at low redshift, but they get fainter with increasing redshift more rapidly than those. This is the reason why in magnitude limited optical samples late type galaxies with redshifts $z \geq 0.5$ are very rare.

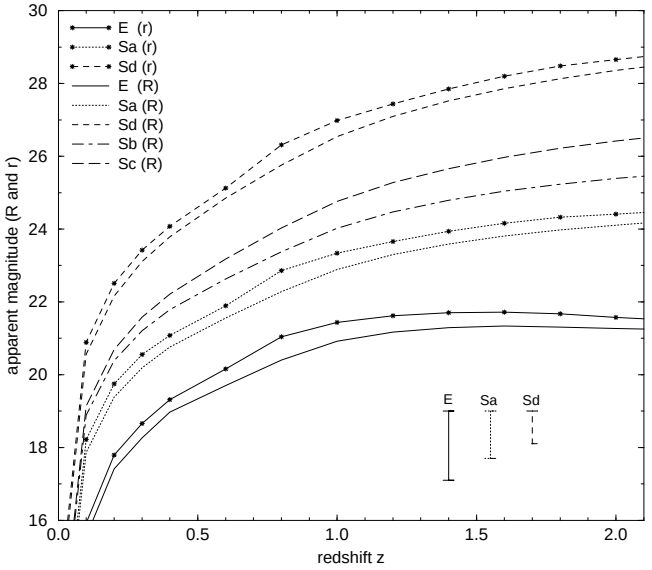

Fig. 1. Results from galaxy evolution models with cosmological parameters $H_0 = 50$ km s^{-1} Mpc^{-1} and $\Omega_0 = 1$ using two different filter response functions: Johnson R and Thuan & Gunn r. Thuan & Gunn r(z) curves are marked with small filled circles. The luminosity range of the various galaxy types as derived from their luminosity functions is indicated in the lower right corner

The redshift evolution of apparent magnitudes for E and Sd models confine the range of normal galaxies from the upper and lower luminosity limit. In an analogous way, the color evolution with redshift of our E and Sd models bracket the color range of normal galaxies from the red and blue, respectively. Observational data are expected to somewhere fall within the region between our E and Sd models. In the lower right corner of Figure 1 we indicate the luminosity range of $\pm\sigma_R$ for galaxies of various Hubble types as derived from Sandage's (1985a&b) luminosity functions.

Figure 1 also shows that over the redshift range from 0.2 to 2 the difference between Johnson's R and Thuan & Gunn's r is approximately constant, $r - R \approx 0.4$, independent of the spectral type.

We find considerable differences in these results for various cosmological parameters H_0 and Ω_0. This is shown in Figure 4 and discussed in §4.3.

We adopt a redshift of galaxy formation $z_{\rm form} = 5$ throughout this investigation. Smaller values seem to contradict observations of very high redshift galaxies (predominantly radio galaxies), and for a larger $z_{\rm form}$ the differences in evolution time for the redshift range $0.2 < z < 2$ are very small and thus do not influence the results considerably. Previous work (Guiderdoni, 1986 and Fritze v. – Alvensleben, 1989) also shows that differences in the results using $z_{\rm form} = 5$ and $z_{\rm form} = 10$ are negligible in the redshift range $0.2 < z < 2$.

3. Data about optically identified QSO absorbers

We have compiled from the literature all available data on observations of optically identified QSO absorption systems. Data have been collected from 17 different publications, details which are important for our purposes are summarized in the appendix (electronically published). A brief overview with the most relevant data for our current investigation is given in Table 1 and is detailed in §3.1.

These data from various authors are very inhomogeneous making the comparison between various data sets as well with results from model calculation rather difficult.

In this work we confine ourselves to the interpretation of magnitudes and colors of the high redshift galaxy sample detected in search for QSO absorbers. A detailed investigation of individual absorbers, also combining chemical information (e.g. column densities, ionisation state, etc.) derived from the absorber imprint on the QSO spectrum with spectrophotometric information obtained for the optically identified absorber will be the subject of a forthcoming paper.

In the following subsections data on apparent magnitudes and redshifts for absorbing galaxies observed by various authors are discussed in more detail.

3.1. Overview

Table 1 gives a brief overview on published observations of optically identified QSO absorber systems. Each record in the Table is labeled with a number we refer to in the text and Figures (column 1). In column (2) we give the author's name and in column (3) the type of absorption system is indicated. The records in the Table are in chronological order. In the next three columns, we list the numbers of observed QSO fields (4), of detected absorption systems (5), and of spectroscopically measured galaxy redshifts (6). In the remaining columns the numbers of apparent magnitudes determined using Thuan & Gunn (1976) filters g (7), r (8), i (9) and Johnson (1966) filters V (10), R (11), K (12), are given. The last column (13) contains some remarks on the specific passbands (filters) used by the authors.

Note that some objects are counted more than once in Table 1, i.e. they may be cited by various authors or

Table 1. Published observations of optically identified QSO absorbers (cf. §3.1.): Number of QSO fields being investigated, number of absorber systems (column "z_{abs}"), number of spectroscopically measured galaxy redshifts (z_{gal}) and apparent magnitudes (Thuan/Gunn, Johnson or others) in the literature

id. no.	author	absorber	QSOs	z_{abs}	z_{gal}	g	r	i	V	R	K	filter
(1)	(2)	(3)	(4)	(5)	(6)	(7)	(8)	(9)	(10)	(11)	(12)	(13)
1)	Lanzetta & Bowen, 1990	MgII	13	16	0	0	[1)]14	0	0	0	0	r band, m_r
2)	Yanny *et al.*, 1990	MgII	8	8	8	0	0	0	0	[2)]37	0	R, div.
3)	Bergeron & Boissé, 1991	MgII	19	21	16	0	**21**	0	**9**	0	0	$m(r)$,m_r, m_V
4)	Bechtold & Ellingson, 1992	MgII	10	2	34	0	34	0	0	0	0	r, m_r
5)	Bergeron *et al.*, 1992	MgII	2	4	5	0	**6**	**6**	0	0	0	r band, r, Gi
6)	Nelson & Malkan, 1992	MgII	18	19	6	43	0	0	0	0	0	Gunn g
7)	Steidel & Dickinson, 1992	MgII	1	3	6	**6**	0	**6**	0	**6**	0	g, $\mathcal{R}$, i , (AB)
8)	Steidel & Hamilton, 1992	div.[3)]	1	2	0	2	0	0	0	2	0	U_n, G, $\mathcal{R}$, (AB)
9)	Yanny & York, 1992	MgII	3	3	0	0	0	0	**3**	**7**	0	R
10)	Drinkwater *et al.*, 1993	MgII	21	24	0	0	0	0	0	25	0	R
11)	Le Brun *et al.*, 1993	MgII	12	17	6	0	24	0	0	0	0	r band, m_r
12)	Spinrad *et al.*, 1993	div.[3)]	1	9	8	**7**	**9**	0	0	0	0	Gunn g, r
13)	Steidel *et al.*, 1993	—[4)]	1	1	2	0	0	**2**	0	**2**	0	$\mathcal{R}$, i , (AB)
14)	Aragon-Salamanca *et al.*, 1994	CIV	10	[5)]10	0	0	0	0	0	**9**	**19**	R, K
15)	Ellingson *et al.*, 1994	CIV	10	4	1	0	7	0	0	0	0	Gunn r
16)	Steidel *et al.*, 1994a	DLA	1	1	0	0	0	0	0	**1**	**1**	$\mathcal{R}$, K, (AB)
17)	Steidel *et al.*, 1994b	DLA	2	3	0	0	0	**3**	0	0	**2**	I_{AB}, K_S

Notes: [1)] $z_{abs} > 14$: For some absorption systems no galaxy was found. [2)] For 14 from the 37 objects only lower limits are given. Confirming spectroscopy for 8 galaxy redshifts is taken from Yanny (1990). [3)] Diverse absorber systems (Lyα, CIV and MgII) have been observed. [4)] An absorption system will be searched for the dwarf galaxy (cf. appendix 13)). [5)] Mean value from multiple absorption systems was taken (cf. appendix 14)).

else, a specific galaxy can be a possible absorber candidate to more than one absorption system. This means that the number of physically different objects is somewhat smaller than the total number of objects in Table 1.

3.2. Redshift data

In column (5) of Table 1 we list the number of absorption systems in the respective QSO spectrum and in column (6) the number of spectroscopically measured galaxy redshifts is given. Usually more than one absorption line system is known for a single QSO spectrum. Thus in many cases the number of absorption redshifts is larger than the number of QSO fields being investigated.

Zero values in column (6) (7 occurrences in Table 1) indicate investigations without spectroscopically measured redshifts. In these cases statistical methods are used to identify the most probable absorber candidate from the image of the QSO environment. Often more than one galaxy are possible candidates for a given absorption line redshift z_{abs}.

Less galaxy redshifts than absorption systems reported in Table 1 means that spectroscopy was not done for all possible absorber galaxies or that no galaxy was found at the appropriate redshift. If the number of galaxy redshifts (column "z_{gal}") is larger than that of absorber redshifts (column "z_{abs}") more than one absorber candidate was investigated spectroscopically. In this case some galaxies with $z_{gal} \neq z_{abs}$ are in the sample which are not absorbers. Otherwise, i.e. if $z_{gal} = z_{abs}$ for more galaxies than absorption line systems, two ore more galaxies could cause the absorption indicating a small group of galaxies or remote parts of a cluster in the line of sight to the QSO.

Spectroscopic redshifts are of course the most reliable data, but such measurements are not always available and then redshifts are inferred from the assumption that the galaxy in the field closest to the QSO gives rise to the absorption line system observed at z_{abs} and thus the redshift is as uncertain as the absorber identification. Therefore we use two different "reliability classes" for all $m(z)$ data distinguishing between galaxies with *spectroscopically confirmed redshifts* (**filled symbols** in Figures 2 – 4) and *possible candidates* without spectroscopic redshift confirmation (**open symbols** in Figures 2 – 4).

3.3. Apparent magnitudes

Table 1 shows that the set of apparent magnitudes measured for optically identified absorbing galaxies is extremely inhomogeneous. This is a crucial problem for the comparison of Johnson R and Thuan & Gunn r magnitudes are most widely used (altogether 204 occurrences in Table 1), measurements in other passbands are rarer (56 g–, 16 i–, 9 V–, 22 K–magnitudes).

Even more scarce is information about colors, i.e. measurements in more than one photometric band. 9 $(V-r)$, 6 $(r-Gi)$, 6 $(g-i)_{\rm AB}$, 6 $(g{-}\mathcal{R}_{\rm AB})$, 7 $(\mathcal{R}\text{-i})_{\rm AB}$, 7 $(g-r)$, 10 $(R-K)$ and 2 $(I_{\rm AB}-K_s)$ colors are given or can be derived from available magnitudes. Observations in more than one passband are emphasized by bold numerals in Table 1. Some authors give one apparent magnitude and one color, then the second magnitude is derived from the color.

As shown in Figure 1 and discussed in §2.2. we may safely adopt the relation $r-R \approx 0.4$ to transform all r band observations to Johnson's R for the purpose of comparison with our galaxy evolution models. However, relations of this kind cannot be generalized because they depend not only on the shape of the filter response function but also on the specific galaxy spectrum. Transformations from one photometric system into another as e.g. given in Landolt–Börnstein VI/2b (1982) cannot be used at redshifts $\neq 0$ for the same reason.

More troubling than the great variety of filter systems is the fact that some authors do not give detailed information on the photometric system they use. We adopt Gunn r if "r band", "r", "m_r" or "m(r)" is mentioned in the text (cf. also column (13) in Table 1) and Johnson R in case of "R" or "m_R".

Some investigators give maximum transmission wavelength λ_0 and FWHM $\Delta\lambda$ of the filter they use. For instance, Steidel *et al.* throughout use a red filter named $\mathcal{R}$ characterized by $\lambda = 6930$ and $\Delta\lambda = 1500$ (e.g. Steidel & Dickinson, 1992). Steidel & Hamilton (1993) plot the filter response function of their (U_n, G, $\mathcal{R}$) photometric system and argue that $\mathcal{R}$ is close to the original Johnson R. Thus we adopt the rough approximation $\mathcal{R} \simeq$ R to include Steidel *et al.*'s data in our compilation.

With the appropriate filter functions our synthetic galaxy spectra can easily be convolved to give magnitudes in any photometric system. This will be done in a forthcoming paper investigating individual objects in more detail.

Some authors (cf. Table 1) use AB magnitudes as established by Oke & Gunn (1983). According to Lilly *et al.* (1991) who give approximate transformations to Johnson's system for B, V and I ($B \sim B_{\rm AB} + 0.17$, $V \sim V_{\rm AB}$ and $I \sim I_{\rm AB} - 0.48$) we derive $R \sim R_{\rm AB} - 0.25$ using the F–type sub dwarfs tabulated by Oke & Gunn (1983) together with Johnson's (1966) colors.

3.4. Summary

For the first time an attempt was made to compile all the currently available observational data on optically identified QSO absorber systems. Our main goals are:

- We would like to establish the status quo of absorber galaxy data as a basis for further completion of the sample.
- We want to demonstrate the usefulness of this sample for the comparison with evolutionary models for galaxies. In particular, we study the Hubble diagram for our models together with observational data from this sample.

Some important properties of a sample of optically identified QSO absorber galaxies should be repeated here:

- ◦ Because selection is done with respect to gas absorption cross section (cf. Steidel, 1993) this sample is almost unbiased with respect to luminosity, surface brightness, radio emission, etc.
- ◦ The search for QSO absorbers provides optical data on a large number of normal galaxies at high redshift. Usually the number of galaxies found is higher than the number of absorbers searched for, i.e. neighboring objects or galaxies at somewhat lower or higher redshift are found in the same field. Their observed properties are almost as valuable as the "true" absorbers for the study of evolutionary effects in galaxies and for possible constraints on cosmological parameters.

However, the compilation of our sample from different sources is connected with some problems:

- ⋆ Inhomogeneity of data, e.g. various authors give apparent magnitudes in different passbands and use different photometric systems.
- ⋆ Detailed information on the photometric system (filters and calibrations) is often very difficult to retrieve.
- ⋆ From most sources apparent magnitudes are available in one passband only, i.e. no color information is available.

We hope that this pilot study will help continue observations to not only identify absorbers but also provide as much information (colors) as possible for a more detailed comparison with galaxy evolution models.

4. Comparison with models

In this Section we compare the data from published observations described in §3 with the results from our galaxy evolution models described in §2 using a standard set of cosmological parameters ($\rm H_0 = 50\ km\ s^{-1}\ Mpc^{-1}$, $\Omega_0 = 1$ and $\Lambda_0 = 0$).

Because of the inhomogeneity and scarcity of published data (as discussed in §3) we restrict our comparison with galaxy evolution models to apparent magnitudes R(z), r(z) and g(z) and colors (g–r)(z).

various publications are distinguished by different symbols. **Filled** symbols indicate *spectroscopically confirmed* redshift data whereas **open** symbols mark *less reliable* absorber *candidates*. Spectroscopically measured redshifts for non absorber galaxies are marked with bold open symbols. We emphasize that the distributions of filled and open symbols are rather similar indicating no systematic deviations of data for confirmed and candidate absorbers. Results from galaxy evolution calculations are presented as curves with different line–type for respective spectral types (indicated as E . . . Sd at the curves). Luminosity ranges (2σ bars), i.e. deviations from the model curves, for types E, Sa and Sd are given in the lower right corner as in Figure 1

4.1. General presentation and results

In Figure 2 we present data on apparent red magnitudes in the Johnson R band as a function of redshift z. Data in the Thuan & Gunn r band have been transformed according to $R = r - 0.4$ as discussed in §2.2. The whole data set presented was taken from 14 different sources. Data points from each publication are marked with different symbols and the numbers in the legend correspond to the references listed in Table 1. Data from papers 1), 6) and 17) do not appear in Figure 2. All observations reported in 1) (Lanzetta & Bowen 1990) are covered by later publications, predominantly by Bergeron & Boissé (1991). Nelson & Malkan (1992) – paper number 6) – and Steidel *et al.* (1994b) – paper number 17) – did not publish any r or R magnitudes.

According to our two "reliability classes" introduced in §3.2., **filled symbols** correspond to galaxies with *spectroscopically confirmed redshifts* and **open symbols** denote *less reliable* absorber *candidates*. Some galaxies turned out to be not the absorber after spectroscopy had been performed. Thus as a third class of objects we have to consider *spectroscopically confirmed non–absorber galaxies*. They are marked with an "bold open symbol" in Figures 2 and 4.

The results from our evolutionary spectral synthesis code are presented, too. Figure 2 shows 6 curves for various spectroscopic galaxy types E, S0, Sa, Sb, Sc and Sd, as characterized by their respective star formation laws (see §2.1.).

An important result immediately seen from Figure 2 is that virtually all observational data points are lying between the curves for E– and Sd–models. Taking into account the luminosity ranges of the various galaxy types ($2\sigma_R$ bars in the lower right corner of Figure 2) as derived from their respective luminosity functions we can state that all data are bordered by our model curves for E– and Sd–galaxies and accordingly we can establish global conformity between our galaxy evolution models and observational data.

Apparent g–magnitudes g(z) from two references along with the respective model calculations for the same standard set of cosmological parameters are presented in Figure 3 a). This representation of the Hubble diagram confirms our results for r– and R–magnitudes. Nearly all g–magnitudes lie in the region confined by our E– and Sd–curves, however, the number of data points is much smaller than in Figure 2. Some absorber *candidates* from Nelson & Malkan (1992) (cf. reference 6) in Table 1) marked as open circles in Figure 3 a) seem to be brighter than our E–curve even when the intrinsic luminosity scatter (indicated by the bar at the E–curve) is taken into account. However, redshifts of these objects are not measured spectroscopically but inferred from the assumption that they are at the redshift of the QSO absorption system. If spectroscopy would not confirm the high redshifts of these objects but instead place them at lower redshift, they might come to lie within the range of our models. We note that all $g(z)$ data with *spectroscopically measured* redshifts are instead bracketed by our models.

Observational data on apparent magnitudes in other passbands (e.g. i, V) yield similar results but are not discussed any further here because of the small number of data points available.

In Figure 3 b) (g–r) color evolution is presented with data from the same references as in Figure 3 a) because they provide the most comprehensive set of color data available so far (cf. Table 1). In both figures numbers are assigned to the data points to identify each individual absorber galaxy for further discussion.

(g–r) colors of all our model galaxies (E through Sd) get redder by about the same amount towards higher redshift until $z \sim 0.5$ and bluer thereafter. The reason for this behavior is that for $z < 0.5$ the cosmological correction $k_\lambda(z)$ dominates the evolutionary correction $e_\lambda(z)$ for E–galaxies while for $z > 0.5$ the contrary is true. For the Sd–model with its SF rate being constant in time, $e_\lambda(z)$ is always very small. $k_\lambda(z)$ (hereafter k_g) for the g band increases by ~ 0.7 mag from $z \sim 0$ to $z \sim 0.4$ with k_r ($k_\lambda(z)$ for the r band) still remaining negligible. This explains the reddening of Sd galaxies for z going from 0 to ~ 0.4. Between $z \sim 0.6$ and 0.8, k_r increases to ~ 0.6 with k_g remaining close to its $z \sim 0.4$ value. This accounts for the bluing of (g–r) for $z > 0.4$.

Colors are more useful than luminosities for the comparison of models with observations, especially if they cover a long wavelength range, and thus, in particular, more color data would be desirable.

4.2. Evidence for late type absorber galaxies

Figure 2 suggests that all spectral types of galaxies from E through Sb and possibly all through Sd are present within the sample of optically identified absorber galaxies. Most of the absorber galaxies appear to be early through intermediate type spiral types (Sa–Sbc) but many ellipticals and late spirals seem to be present, too. For instance two absorber candidate objects from Yanny *et al.* (1990) (reference 2) in Table 1 and small circles in Figure 2) fall very close to the Sd–curve.

Figure 3 a) which shows g–magnitudes for the same models as Figure 2 reveals one spectroscopically confirmed object (number 3 in Figure 3 a)) fairly close to the Sd–curve but the color of this object in Figure 3 b) rather suggests an early spiral type.

Roughly, from the g(z) – diagram in Figure 3 a) we would tend to attribute an early type to objects 2 and 6,

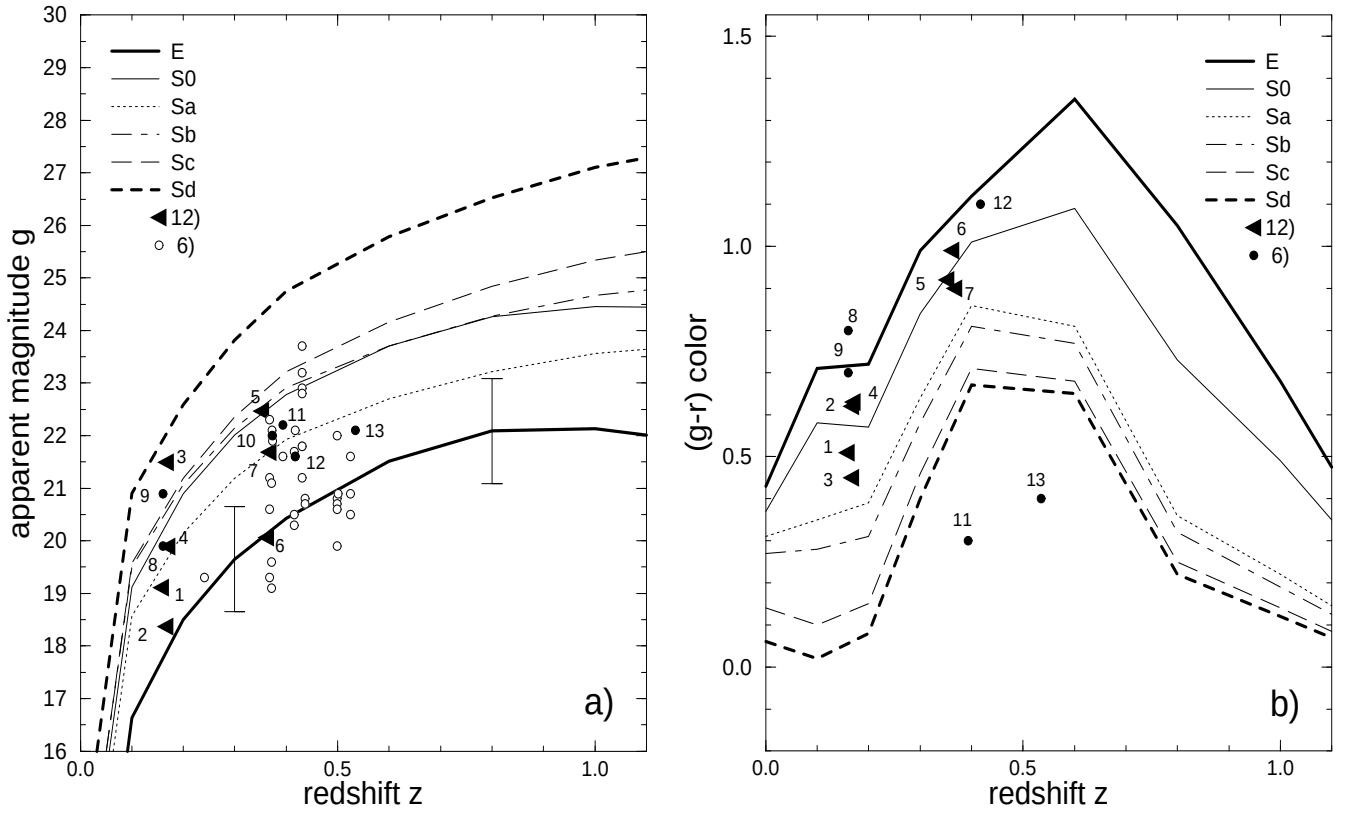

Fig. 3. a) Comparison of observed g(z) data with galaxy evolution models. Hubble types and references of observations are indicated in the legend. b) (g–r) colors for the same references and models as in a). All redshifts for (g–r)(z) data points (refer. no. 6) and 12) from Table 11) have spectroscopically confirmed. Data points are given the serial numbers in both panels to identify objects for further discussion in the text.

Fig. 4. Comparison of observational data with our galaxy evolution models for different cosmological parameter pairs (Ω_0, λ_0) with H_0 = 100 km s^{-1} Mpc^{-1}: a) (0.5, 0.1), b) (1, 1), and c) (1,0.1). For (0.5, 1) we refer to Figure 2. Note that the data points are always the same.

an intermediate type to objects 4, 5, 7, 8, 10 and 11 and a late type to object 3.

From the color–redshift diagram (g–r)(z) in Figure 3 b) we would confirm the early type object classification of objects 2 and 6 and the intermediate type classification of objects 4 and 5. However, object 8 is too red to be consistent with our luminosity – based type classification, and objects 11 and 13 are much too blue. For object 10 no r–magnitude and thus no (g–r) color is available.

A more detailed investigation of the individual objects is required to decide about the nature of those few objects which are either too blue or too red to be explained by our model curves. Our models describe average spectral types of normal isolated galaxies and are not capable to explain these peculiar objects. Additional reddening might be explained by internal dust and the very blue colors could be due to a burst of star formation perhaps in the course of galaxy interaction or the presence of an AGN.

As a word of caution it should be mentioned that even a galaxy with a redshift $z_{gal} \approx z_{abs}$ cannot be proven to be the actual absorber, there can always be a fainter source with still closer projected distance to the quasar that is not detected. However, as long as those – probably very few – objects in Figure 2 and 3 that are not the physical absorbers, do not have systematically different luminosities and colors from the real absorbers, our conclusions remain valid.

The presence of intermediate and late type galaxies among QSO absorbers is to some degree unexpected and has far–reaching consequences. The first MgII–absorbers that had been optically identified by Bergeron & Boissé (1991) were ∼L* galaxies with luminosities brighter than those of intermediate/late type galaxies.

The presence of intermediate and late spectral types among QSO absorbers, if confirmed by future observations, would imply that at least an important fraction, if not all, of these galaxies do have extended gaseous halos with Mg– and C–column densities high enough to cause absorption stronger than the lower limit equivalent width for the detection of an absorption feature. Detailed investigation of individual objects – both from a chemical and from a spectroscopical point of view – promise interesting results for masses and extensions of halos (as derived from impact parameters), dark matter content of galaxies and chemical evolution scenarios. These objects will be an

exciting target for HST imaging as well as a challenge for chemical and dynamical evolution models.

Unfortunately, almost no information about spectral or morphological types is as yet available for the optically identified QSO absorbers. Figure 2 can be understood as to predict – within the uncertainties given by the partly overlapping luminosity ranges of the different galaxy types – the spectral types of individual absorbers. These predictions can directly be tested by spectral observations, which, however, for these faint objects, requires longer integration times than those generally applied to just obtain a redshift.

If the direct relation between spectral and morphological type observed for nearby galaxies would extend to high redshifts, then Figure 2 could be used to predict morphological types for individual absorbers. Deep HST imaging should allow to assess this interesting question for redshifts up to $z \sim 0.5$.

Interestingly, Dickinson (1995) reports recent HST observations of the $z = 0.44$ absorber in front of 4C06.41 which directly reveal a spiral morphology. This observation is part of a large optical identification project of MgII absorbers which may reveal more such exciting results in the near future. Further evidence for extensive dark halos around two nearby ($z = 0.092$ and 0.075) low–luminosity spiral galaxies inferred from QSO absorption line studies was reported by Barcons *et al.* (1995). However, data are still scarce and this conclusion remains to be confirmed by future observations.

4.3. Discussion of cosmological parameters

Our galaxy evolution models enable us to study the influence of different parameters (H_0, Ω_0) in the standard Friedmann–Lemaître cosmology. We consider four different parameter combinations (h, Ω_0) of the Hubble constant ($H_0 = 100$ h km s^{-1} Mpc^{-1}) and the density parameter Ω_0 in the Hubble–diagram for red apparent magnitudes R(z).

(h, Ω_0) = (0.5, 1) is already shown in Figure 2 and the parameter combinations (0.5, 0.1), (1, 1) and (1, 0.1) are presented in Figure 4 panels a) to c). Only our E–, Sa– and Sd–models are depicted for clarity.

In the case of $H_0 = 50$ km s^{-1} Mpc^{-1} and $\Omega_0 = 0.1$ (Figure 4 a)) a large number of galaxies are by up to two magnitudes brighter than the E–galaxies in our model. In other words, calculations with this cosmological model result in galaxies much too faint as compared with the observations. Thus, the combination of $H_0 = 50$ km s^{-1} Mpc^{-1} with a low cosmological density parameter $\Omega_0 = 0.1$ cannot be reconciled with the data.

Not for ellipticals but for spectral types S0 and later, gaseous emission and internal extinction do affect observed magnitudes. These effects are not included in our models but have been studied by Guiderdoni & Rocca–Volmerange (1988). They find that over a range in redshift $z = 0 \ldots 2$ and in wavelength from V through I nebular emission does at most brighten a galaxy by 0.1 mag, while internal extinction can significantly dim early spiral types (e.g. by ~ 0.5 mag in V and ~ 0.4 mag in R for S0's at $z \sim 1.6$ cf. Guiderdoni & Rocca–Volmerange (1988), seen at random orientation and less for later spectral types and/or different redshifts).

Figure 4 b) and c) show similar comparisons in the case of $H_0 = 100$ km s^{-1} Mpc^{-1}. In both cases, $\Omega_0 = 1$ and $\Omega_0 = 0.1$, the observations fall fairly well within the envelopes given by the model E– and Sd–galaxies, i.e. in combination with a high value for H_0 both high and low density parameters seem to be compatible with the data. In a later investigation with more data on colors available we hope to be able to put further constraints on cosmological parameters.

The difference in luminosity evolution between high and low cosmological density which we find in our models for early type galaxies is larger than the one reported in earlier work by Guiderdoni & Rocca–Volmerange (1987) and others using Bruzual's models (e.g. Spinrad & Djorgovski, 1987). For instance at a redshift of 2, our low Ω_0 E–model predicts $m_R \simeq 24.3$ while for $\Omega_0 = 1$ we find $m_R \simeq 21.3$. This large difference is due to the fact, that we use more recent stellar evolutionary tracks from the Geneva group. Interestingly, our results agree quite well with those of Bressan *et al.* (1994) who use a recent set of stellar tracks from the Padova group, reflecting the fact, that over the last years, these independent approaches of stellar evolutionary modeling have converged to large extent. Most important changes have occured for low–mass stars, explaining why towards later spectral types the differences to earlier models get much smaller.

The Sd model with its constant SF rate only shows little evolution, the cosmological corrections, too, are small, and both largely compensate for each other. Thus, the magnitude difference between models for $\Omega_0 = 1$ and $\Omega_0 = 0.1$ is dominated by the difference of the bolometric distance module for both cases.

For illustrative purposes we chose to present here the extreme values $H_0 = 50$ km s^{-1} Mpc^{-1} and $H_0 = 100$ km s^{-1} Mpc^{-1} discussed today. We have, of course, examined a large variety of combinations of parameters H_0, Ω_0 and $z_{\rm form}$. At this preliminary stage, we only briefly want to state that for $H_0 = 75$ km s^{-1} Mpc^{-1} a density parameter as low as $\Omega_0 = 0.1$ seems to be excluded by the data. $\Omega_0 = 0.5$ is marginally allowed, provided that the absorber at $z \approx 1$ (cf. Figures 2 & 4) and the candidates at $z \approx 1.67$ and $z \approx 1.79$ are all from the high luminosity tail of the elliptical galaxy luminosity function. Density parameters $\Omega_0 > 0.5$ to $\Omega_0 = 1$ are easily compatible with all available data.

We have also studied models with a Salpeter–IMF and find that this would not alter our conclusions concerning cosmological parameters. It does make galaxies brighter by a constant value of ~ 1 mag both in V and R over all

times from 2 through 16 Gyr without changing the colors. As galaxies at their present age – as given by (H_0, Ω_0, $z_{\rm form}$) – are normalized to mean Virgo luminosities this constant brightening drops out over the whole redshift range from $z = 0 \ldots 2$. Only if the IMF would be allowed to significantly change with time, it might change our conclusions.

5. Discussion

5.1. Problems with observational data

The compilation of apparent magnitude and color data as a function of redshift for optically identified QSO absorber galaxies is rendered more difficult by two main problems.

First, various authors use **different photometric systems** and do not always give all the **information on filters and calibrations** necessary for our attempt to compile data from various investigators into one large comprehensive data base. This makes it difficult to compare data from different publications with our results from galaxy evolution models. As a first approach we use rough transformations between different photometric systems as discussed in §3.. Because most of the present data are given in the Johnson or Thuan & Gunn filters we restricted our comparison to these two photometric systems, but we stress, that in principle, apparent magnitudes can easily be calculated from model spectra for any photometric system if the filter functions are known as discussed in §2. This will be done in future projects intended to study individual objects in detail where more accurate data will be necessary.

The second main problem concerns the **determination of redshifts if no spectroscopic data are available**. Thus in §3.2., we divided the redshift data in two "reliability classes" (*spectroscopically confirmed* and *candidates*). Objects with spectroscopic redshifts, however, do seem to show the same distribution in our Hubble diagrams for R and g as those for which the redshifts were only estimated. In many cases the absorber galaxy cannot be clearly identified, i.e. several "possible candidates" are discussed because more than one galaxy is close to the QSO sight line. In these cases more than one absorber candidate is given for some particular redshift and the real physical absorber cannot be identified. In these cases we include several candidates in Figure 2, 3a) and 4 (symbols with exactly the same z value) to see if any of them lie outside the ranges of our model curves. It seems improbable that the "true absorbers" should deviate systematically in luminosity or color from those galaxies that do not cause the absorption but lie close to the absorber both in redshift and projected separation. Another possibility is that more than one galaxy contributes to the absorption system, i.e. there is a group or cluster of galaxies.

5.2. Groups and clusters of galaxies

The number of spectroscopically measured galaxy redshifts does not need to be equal to the number of confirmed optically identified QSO absorbers. On the one hand, the redshifts $z_{\rm abs}$ and $z_{\rm gal}$ may be different indicating that the respective galaxy cannot be the absorber (open bold symbols in Figure 2) . On the other hand, there may be more than one spectroscopically investigated galaxy with a redshift $z_{\rm gal} \approx z_{\rm abs}$. The latter case indicates a group or the outskirts of a cluster of galaxies, whereas either only one galaxy, probably the closest to the line of sight, or the halos from the members of a group or cluster may be responsible for the absorption system.

For instance, in Figure 3 a) objects 1 to 4 from Spinrad *et al.* 1993 (reference 12 in Table 1) nearly have the same (spectroscopically measured !) redshift $z \approx 0.17$ and thus seem to be members of a small group or part of a cluster. However, no answer can be given to the question, which galaxy (or galaxies) from this group actually causes the absorption lines. This might even affect our tentative identification of an Sd galaxy absorber (object 3 in Figure 3 a)).

6. Future prospects

The purpose of this study was to compile a comprehensive sample of galaxies detected in various attempts to optically identify QSO absorbers and to compare them to our galaxy evolution models. In this first approach we studied Hubble diagrams for apparent magnitudes R and g as well as color vs. redshift relations using all galaxies found, i.e. confirmed absorbers as well as candidates.

In further studies, we intend to investigate the extension and chemical composition of galaxy halos for selected individual objects in more detail together with spectrophotometric properties. Data on impact parameters and rest–frame equivalent widths are already available for most published objects.

Furthermore our evolutionary spectral synthesis code can be extended for comparison with observations in the K band using new stellar spectral libraries. Additionally, our models can be calculated for different metallicities, especially subsolar ones that may be better suited for late type galaxies at high redshift in an attempt to consistently understand chemical abundances of the halo gas as well as the spectrophotometric appearance of the visible part of the galaxies.

7. Conclusions

Optically identified QSO absorption systems as well as non–absorbing galaxies serendipitously detected in these deep fields provide a nearly unbiased sample of field galaxies with high redshifts. A comprehensive set of data on

those galaxies has been compiled from the literature and is compared with results of our galaxy evolution models.

- This is the first attempt to put together a compilation of all observational data currently available on optically identified QSO absorption systems. Care is taken to compare observations made in different filter systems to establish a basis for future applications and further completion of the sample.
- For a standard cosmological model ($H_0 = 50$ km s^{-1} Mpc^{-1}, $\Omega_0 = 1$, $\Lambda_0 = 0$) and a redshift of galaxy formation $z_{\rm form} = 5$, we find good agreement between our galaxy evolution models and observed apparent magnitudes and colors over a large redshift range ($0 \leq z \leq 2$).
- All spectroscopic galaxy types seem to be present in the sample of absorber galaxies with the bulk of the absorbers being of early and intermediate spiral types. However, even late type spirals seem to cause absorption lines in QSO spectra. The correspondence between spectral and morphological galaxy types at high redshift remains to be investigated, though first observations at $z \sim 0.5$ seem to favor it.
- If confirmed, the fact that intermediate and late type galaxies also cause absorption in QSO spectra has far–reaching consequences for the sizes and chemical enrichment of their halos and for the dark matter content.
- A combination of cosmological parameters $H_0 = 50$ km s^{-1} Mpc^{-1} and $\Omega_0 = 0.1$ can be excluded from a comparison of the data with our models. For a Hubble constant $H_0 = 100$ km s^{-1} Mpc^{-1}, both high and low density parameters $\Omega_0 = 1$ and $\Omega_0 = 0.1$ might be admitted by the data.
- Colors of optically identified absorber galaxies are very scarce and, thus, do not allow for any further conclusions. **More data in two or more passbands** are needed for further detailed studies of cosmological models.

We caution again that the results presented here depend on our adopted models and on the input physics used. Both might be better constrained in the near future.

Acknowledgements. This work was supported by Verbundforschung Astronomie/Astrophysik through BMFT grant FKZ 50 0R 90045 and by the DFG through grant Fr316–1. We thank the anonymous referee and Prof. Dr. J. Lequeux for their suggestions that helped to improve the presentation of our results.

Appendix : Notes on individual publications

In the following we briefly comment on each paper from which we have compiled data. Numbers of sub-subsections (1) ... 17)) correspond to the identification number (id. no.) in Table 1 and Figures 2 – 4 as well. In particular we discuss some points which are important to our purposes.

1) Lanzetta & Bowen 1990

In their paper entitled *Intermediate redshift galaxy halos: Results from QSO absorption lines* K.M. Lanzetta and D. Bowen list optically identified MgII absorption systems in their TABLE 1 for the purpose to study correlations between equivalent widths of MgII absorption lines and impact parameters. We assume that TABLE 1 in this paper contains all data on optically identified (MgII) absorption systems available up to this time and thus we take it as the starting point for our search for further data in the literature until now. All $m_r(z)$ data listed in TABLE 1 are reported also in later papers and we took them from these more topical sources.

2) Yanny *et al.* 1990

In their paper entitled *Emission–line objects near QSO absorbers. I. Narrow–band imaging and candidate list* B. Yanny, D.G. York and T.B. Williams report on a search for emission–line objects (predominantly from [OII]) in the environment of 8 QSOs with previously known associated MgII absorber systems using narrow–band imaging. Data for 37 objects are given but in 14 out of the 37 cases only lower limits for R magnitudes could be derived from the detection limit.

In a subsequent study (Yanny 1990) 8 of the 37 absorber candidates in 4 QSO fields have been investigated using long–slit spectroscopy confirming their incidence with the absorber redshifts ($0.4 \leq z_{\rm abs} \leq 0.7$). It turns out that all 8 spectroscopically studied objects are absorbers, i.e. $z_{\rm gal} = z_{\rm abs}$.

3) Bergeron & Boissé 1991

In their paper entitled *A sample of galaxies giving rise to* MgII *quasar absorption systems* J. Bergeron and P. Boissé present imaging and spectroscopic observations aimed at detecting intervening galaxies responsible for low redshift ($z \sim 0.5$) MgII absorption line systems in quasar spectra. This paper represents a pioneering study on optical identifications of absorber systems confirming the intervening galaxy hypothesis. 14 confirmed identifications, 4 candidates and 3 "negative cases", i.e. galaxies closest to the QSO line of sight but without any absorption system at galaxy redshift are presented. The authors give luminosities of galaxies as well as sizes and shapes of the absorbing regions.

We include the 14 spectroscopically confirmed absorber galaxies and 4 candidates in Figure 2 and 4. The three "negative cases" from their Table 6 are included as "candidates" as well.

4) Bechtold & Ellingson 1992

In their paper entitled MgII *absorption by previously known galaxies at* $z \approx 0.5$ J. Bechtold and E. Ellingson

report on an investigation of 9 QSO spectra using the Multiple Mirror Telescope to search for MgII absorption from intervening galaxies. This is the reverse procedure: galaxies and their redshifts ($0.2 \leq z \leq 0.7$) are known from previous studies of the QSO environment and now, the possible absorption systems are searched for. These data are as useful to us as those from studies aimed to find intervening galaxies near QSOs with absorption line systems.

It should be noted that a considerable fraction of the data comes from galaxies in high density environment, i.e. galaxy clusters. This is reflected by the fact that many redshift values are close each other. In the cases where $z_{gal} \neq z_{QSO}$ is not confirmed by spectroscopy a physical influence on the galaxies from the quasar cannot be excluded.

In their TABLE 4, the authors give r(z) data for 21 galaxies in the environment of 9 quasars. Photometric data are taken from Green & Yee (1984), Yee, Green & Stockman (1986), and unpublished images from Yee. Spectroscopy is from Ellingson, Green & Yee (1991) and Ellingson & Yee (1992). Only two MgII absorption–line systems are identified with corresponding galaxy redshifts. Consequently most of the r(z) data from this paper do not belong to optically identified QSO absorbers and consequently they are not included to our compilation.

In TABLE 5 of their paper the authors list previously known identified absorber galaxies (most from Bergeron & Boissé 1991) and some new candidates. The latter ones are included in our compilation.

5) Bergeron *et al.* 1992

In their paper entitled *Discovery of $z \sim 1$ galaxies causing quasar absorption lines* J. Bergeron, S. Christiani and P.A. Shaver report on the first identification of intervening galaxies responsible for four MgII absorption–line systems at redshifts of about 1 in two QSO fields. There are three candidates in each field assumed to be responsible for the MgII doublets in the QSO spectra. Five galaxy redshifts have been measured showing incidence with three of the four absorption line redshifts. Two galaxies are not at any absorber redshift and one galaxy without measured redshift is assumed to be at the remaining absorption redshift. The two confirmed non–absorbers are marked with open bold line symbols in Figure 2.

6) Nelson & Malkan 1992

In their paper entitled *A photometric search for* [OII] *lines in* MgII *quasar absorption systems* B.O. Nelson and M.A. Malkan report on results obtained by narrow– and broad–band photometry of 336 objects near the line of sight to 22 quasars showing MgII absorption lines in their spectra. The attention is focused to [OII] emission–line objects which are claimed to undergo enhanced star formation and these galaxies are searched for using narrow–band photometry. Gunn g magnitudes for 52 objects are given in their TABLE 4. The corresponding absorber redshift can be derived from their list of observed QSO fields in TABLE 1. Some quasars have not been imaged in the Gunn g bandpass but e.g in "Spinrad Red". These data are not included and finally 43 g magnitudes remain in our compilation.

In 6 cases redshifts of identified galaxies had previously been measured spectroscopically by other authors (Bergeron & Boissé 1991, Bergeron *et al.* 1988, Christiani 1987, Miller *et al.* 1987, see also references in TABLE 4 of Nelson & Malkan). In most other cases (without spectroscopy) more than one candidate is given for each absorber redshift. They are all included in our compilation. In five cases we are able to adopt r magnitudes from the papers mentioned to derive (g-r) colors. These colors are used in Figure 3b.

7) Steidel & Dickinson 1992

In their paper entitled *The unusual field of the quasar 3C 336: Identification of three foreground* MgII *absorbing galaxies* C.C. Steidel and M. Dickinson present imaging and spectroscopic observations of the field of 3C 336 ($z_{em} = 0.927$) which reveals at least 3 MgII absorption systems with $z_{abs} < z_{em}$. Data for 6 galaxies with spectroscopically measured redshifts and $\mathcal{R}$ ($\lambda = 6930$, $\Delta\lambda = 1500$), g ($\lambda = 4900$ and $\Delta\lambda = 700$) and i ($\lambda = 8000$ and $\Delta\lambda = 1450$) AB magnitudes are given in their TABLE 1. 3 galaxies seem to be the absorbing galaxies. 3 further objects with $z_{gal} \neq z_{abs}$ are marked with open bold line symbols in Figure 2 and 4 as usual.

In this paper Steidel & Dickinson give apparent AB–magnitudes $\mathcal{R}_{AB}$ (6930/1500) together with $(g-\mathcal{R})_{AB}$ and $(\mathcal{R}-i)_{AB}$ colors. Because we restrict our comparison of observations with models to Thuan & Gunn and Johnson bandpasses as discussed in §2.2 we cannot take the AB colors from Steidel & Dickinson (1992) into consideration.

8) Steidel & Hamilton 1992

In their paper entitled *Deep imaging of high redshift QSO fields below the Lyman limit. I. The field of Q0000-263 and galaxies at $z = 3.4$* C.C. Steidel and D. Hamilton present results for the first field completed in a new survey involving very deep imaging of the fields of high redshift quasars with optically thick Lyman limit absorption systems. In their TABLE 1 the authors list U_n, G and $\mathcal{R}$ magnitudes for 33 objects within 30" of Q0000-263 ($z_{em} = 4.106$). The moderately under–luminous galaxy at $z = 0.438$ was previously suggested to be at $z = 3.408$ (Turnshek *et al.* 1991), but now Steidel & Hamilton suggest that the line previously identified as Lyman α is probably [OII]. The $z = 0.438$ and $\mathcal{R} = 22.5$ galaxy is added to our list and is an interesting case for a late type absorber. Another galaxy is assumed to be a candidate for the DLA system at $z = 3.39$.

9) Yanny & York 1992

In their paper entitled *Emission–line objects near Quasi–stellar object absorbers. III. Clustering and colors of moderate–redshift* HII *regions* B. Yanny and D.G. York report on three deep narrow–band images corresponding to [OII] at the redshift of known QSO absorption–line systems which show evidence for enhanced star formation occurring in groups of giant HII regions spread over 100 – 300 h^{-1}kpc. This paper extends their earlier investigation (Yanny *et al.* 1990, cf. 3)). For the three QSOs under study the authors list all galaxies in the field. From these tables we picked up 7 absorber candidates as suggested by the authors.

10) Drinkwater *et al.* **1993**

In their paper entitled *On the nature of* MgII *absorption line systems in quasars* M.J. Drinkwater, R.L. Webster and P.A. Thomas present the results of a large R–band imaging survey of 71 bright ($m_v < 18$) quasars revealing MgII absorption lines in their spectra. For 21 QSO fields possible absorber candidates are found, however, no galaxy redshifts have been measured. A statistical approach is used to identify galaxies likely to be associated with the absorption systems. In TABLE 5 and 7 of their paper the authors give z_{abs} and R magnitudes for possible absorber candidates. For some galaxies two possible z_{abs} are given.

11) Le Brun *et al.* **1993**

In their paper entitled *A deep imaging survey of fields around quasars with* $z < 1.2$ MgII *absorption systems* V. Le Brun, J. Bergeron, P. Boissé and C. Christian report on an imaging survey of 12 fields around quasars with 17 MgII absorption systems in the r band at the CFH telescope. They give a list (Table 3. in their paper) of altogether 19 absorber candidates with 6 galaxy redshifts being spectroscopically confirmed. It turned out that two of them are not absorber galaxies ($z_{gal} \neq z_{abs}$). The authors emphasize that some of the candidates are rather uncertain.

12) Spinrad *et al.* **1993**

In their paper entitled *Hydrogen and metal absorption lines in PKS0405–123 from the halos of low redshift galaxies* H. Spinrad, A.V. Filippenko, H.K.C. Yee, E. Ellingson, J.C. Blades, J.N. Bahcall, B.T. Jannuzi, J. Bechtold and A. Dobrzycki report on HST ultraviolet and ground–based optical spectra of the bright quasar PKS 0405–123 which has two absorption–line systems. Spectroscopically measured redshifts and Gunn g and r magnitudes are given for 9 galaxies. One redshift is very uncertain. The values of galaxy redshifts are grouped near two different absorber redshifts ($z_1 = 0.1670$ and $z_2 = 0.3516$) indicating small groups of galaxies or outskirts of clusters of galaxies.

In the z_2 system only Lyα absorption is observed whereas in the z_1 system metal lines (CIV and probably MgII) are detected as well.

The authors give r–magnitudes and (g–r) colors (Thuan & Gunn (1976) g and r) in their TABLE 1 and thus g–magnitudes can be derived.

13) Steidel *et al.* **1993**

In their paper entitled *A dwarf galaxy near the sight line to PKS 0454+0356: A fading "faint blue galaxy"?* C.C. Steidel, M. Dickinson and D.V. Bowen report on the discovery of a dwarf galaxy at $z = 0.072$ which is only 4" in projection from the line of sight to the quasar . Fortuitously the spectrum of a second galaxy was recorded simultaneously from several moderately strong emission lines revealing $z \approx 0.2$. Here we are not interested in dwarf galaxies and therefore only data from the latter object are included in our compilation. By now no appropriate absorption lines are found in the QSO spectrum. Future observations (using HST) in search of MgII resonance lines would be very meaningful for the study of the gas associated with an intrinsically faint, star–forming dwarf galaxy.

14) Aragon-Salamanca *et al.* **1994**

In their paper entitled *The nature of distant galaxies producing multiple* CIV *absorption lines in the spectra of high-redshift quasars* A. Aragon-Salamanca, R.S. Ellis, J.-M. Schwartzenberg and J. Bergeron demonstrate that luminous L^* galaxies up to $z \simeq 2$ which cause CIV absorption in the spectra of quasars can be detected by deep infrared (K band) imaging.

The authors use a statistical approach to identify the absorbers from photometry alone because at these faint limits spectroscopy is very difficult. A sample of 11 QSOs with clustered CIV absorption line systems is investigated. In some cases, several suitable complexes at different z_{abs} are present within a single QSO spectrum. As the redshift of possible absorbers we take from their TABLE 1 the mean values $\langle z_{abs}^{CIV} \rangle$ weighted by the appropriate rest–frame equivalent width for each system.

A subset of the QSO fields has also been imaged in R and I. Thus, 19 K magnitudes and 9 $(R-K)$ colors are given in TABLE 2 of the paper. From these data we obtain R magnitudes as a function of redshift for 9 absorber candidates.

15) Ellingson *et al.* **1994**

In their paper entitled *Metal–line absorption at* $z_{abs} \sim z_{em}$ *from associated galaxies* E. Ellingson, H.K.C. Yee, J. Bechtold and A. Dobrzycki report on deep optical imaging and limited spectroscopy of 10 fields around quasars with $0.15 < z_{em} < 0.65$ revealing CIV absorption predominantly at the emission redshift of the QSO. The aim of their investigation is not the optical identification of absorber systems but the study of the interaction of quasars with galaxies from the surrounding clusters. Some of their data, compiled in TABLE 2. are also useful to our purposes. We select 7 candidates from their list, one galaxy with spectroscopically confirmed redshift.

We want to caution that the rich cluster environment and the proximity to the quasars might be influential on the evolution of these galaxies.

16) Steidel *et al.* 1994a

In their paper entitled *The z = 0.8596 damped lyman alpha absorbing galaxy toward PKS 0454+0356* C.C. Steidel, D.V. Bowen, J.C. Blades and M. Dickinson present HST and ground–based data on a new DLA system at z_{abs}= 0.8596 along the line of sight to PKS 0454+0356. Optical images were obtained as part of a large survey for galaxies producing MgII absorption line systems, including a very deep $\mathcal{R}$ (6930/1500) image from which we take the $\mathcal{R}$ magnitude as a function of redshift for this galaxy. The authors only gave a faint limit ($K > 20.5$) for the K magnitude.

17) Steidel *et al.* 1994b

In their paper entitled *Imaging of two damped lyman alpha absorbers at intermediate redshift* C.C. Steidel, M. Pettini, M. Dickinson and S.E. Persson report on observing the fields of the QSOs 3C 286 and PKS 1229–021 in the I and K_s bands. Under good seeing conditions they resolve faint galaxy images close to the QSO sight–lines. We adopt I and K magnitudes as a function of redshift for three absorber candidates from this paper.

References

Aragon–Salamanca, A., Ellis, R.S., Schwartzenberg, J.-M., Bergeron, J., 1994, ApJ 421, 27

Barcons, X., Lanzetta, K.M., Webb, J.K., 1995, Nat 376, 321

Bechtold, J., Ellingson, E., 1992, ApJ 396, 20

Bergeron, B., Boulade, O., Kunth, D., Tytler, D., Boksenberg, a., Vigroux, L., 1988, A&A 191, 1

Bergeron, J., Boissé, P., 1991, A&A 243, 344

Bergeron, J., Cristiani, S., Shaver, P.A., 1992, A&A 257, 417

Bressan, A., Chiosi, C., Fagotto, F., 1994, ApJS 94, 63

Bruzual, G.A., Charlot, S., 1993, ApJ 405, 538

Cristiani, S., 1987, A&A 175, L1

Dickinson, Marc, 1995, in "New Light on galaxy Evolution", eds. R. Bender & R. Davis, IAU Symp. No. 171, in press

Drinkwater, M.J., Webster, R.L., Thomas, P.A., 1993, AJ 106, 848

Ellingson, E., Yee, H.K.C., Bechtold, J., Dobrzycki, A., 1994, AJ 107, 1219

Fritze – von Alvensleben, U., 1989, PhD Thesis, University of Göttingen

Fritze – von Alvensleben, U., Krüger, H., Fricke, K.J., Loose, H.-H., 1989, A&A 224, L1

Fritze – von Alvensleben, U., Krüger, H., Fricke, K.J., 1991, A&A 246, L59

Fritze – von Alvensleben, U., Gerhard, O.E., 1994, A&A 285, 751

Fritze – von Alvensleben, 1994, in: "Stellar populations", eds. P.C. van der Kruit & G. Gilmore, IAU Symp. No. 164, Dordrecht 1994

Guiderdoni, B., 1986, PhD Thesis, Université Paris VII.

Guiderdoni, B., Rocca–Volmerange, B., 1987, A&A 186, 1

Guiderdoni, B., Rocca–Volmerange, B., 1988, A&A Suppl. Ser. 74, 185

Gunn, J.E., Stryker, L.L., 1983, ApJ Suppl. 52, 121

Johnson, H.L., 1966, Ann. Rev. Astron. Astrophys., 4, 193

Kennicutt, R.C., 1992, ApJS 79, 255

Krüger, H., Fritze – von Alvensleben, U., Loose, H.–H., Fricke, K.J., 1991, A&A 242, 343

Krüger, Fritze – von Alvensleben, U., Loose, H.–H., 1995, A&A 303, 41

Lanzetta, K.M., Bowen, D., 1990, ApJ 357, 321

Le Brun, V., Bergeron, J., Boissé, P., Cristiani, C., 1993, A&A 279, 33

Lilly, S.J., Cowie, L.L., Gardener, J.P., 1991, ApJ 369, 79

Maeder, A., 1991, A&A 242, 93

Miller, J.S., Goodrich, R.W., Stephens, S.A., 1987, AJ 94, 633

Nelson, B.O., Malkan, M.A., 1992, ApJS 82, 447

Oke, J.B., Gunn, J.E., 1983, ApJ 266, 713

Rocca–Volmerange, B., Guiderdoni, B., 1988, A&A Suppl. Ser. 75, 93

Sandage, A., Binggeli, B., Tammann, G.A., 1985a, AJ 90, 395

Sandage, A., Binggeli, B., Tammann, G.A., 1985b, AJ 90, 1759

Sandage, A., 1986, A&A 161, 89

Scalo, J.M., 1986, Fundam. Cosmic Phys. 11, 1

Spinrad, H., Djorgovski, S., 1987, in "Observational Cosmology", eds. A. Hewett, G. Burbidge & L.Z. Fang, IAU Symp. No. 124, Dordrecht 1987

Spinrad, H., Filippenko, A.V., Yee, H.K.C., Ellingson, E., Blades, J.C. Bahcall, J.N., Jannuzi, B.T., Bechtold, J., Dobrzycki, A., 1993, AJ 106, 1

Steidel, C.C., Dickinson, M., 1992, ApJ 394, 81

Steidel, C.C., Hamilton, D., 1992, AJ 104, 941

Steidel, C.C., 1993, in: Shull, J.M. and Thronson, H.A. (eds.): The Environment and Evolution of Galaxies, 263

Steidel, C.C., Dickinson, M., Bowen, D.V., 1993, ApJ Lett. 413, L77

Steidel, C.C., Hamilton, D., 1993, AJ 105, 2017

Steidel, C.C., Bowen, D.V., Blades, J.C., Dickinson, M., 1994a, MIT Preprint Series No. CSR–94-24

Steidel, C.C., Pettini, M., Dickinson, M., Persson, S.E., 1994b, MIT Preprint Series No. CSR–94-24

Steidel, C.C., 1995, in: G. Meylan (ed.), QSO absorption lines, Proceedings of the ESO workshop on QSO absorption lines held at Garching, Germany, 21. – 24. November 1994, Berlin/Heidelberg 1995

Thuan, T.X., Gunn, J.E., 1976, PASP 88, 543

Turnshek, D.A., Machetto, F., Bencke, M.V. , Hazard, C., Sparks, W.B., McMahon, R.G., 1991, ApJ 382, 26

Wu *et al.* (eds.) 1983, IUE Ultraviolet Spectral Atlas, *NASA* No. 22

Yanny, B., 1990, ApJ 351, 396

Yanny, B., York, D.G., Williams, T.B., 1990, ApJ 351, 377

Yanny, B., York, D.G., 1992, ApJ 391, 569

This article was processed by the author using Springer-Verlag TEX A&A macro package 1992.